Macromolecules

ARTICLE

pubs.acs.org/Macromolecules

Effect of Free Volume on Water and Salt Transport Properties in Directly Copolymerized Disulfonated Poly(arylene ether sulfone) Random Copolymers

Wei Xie,[†] Hao Ju,[†] Geoffrey M. Geise,[†] Benny D. Freeman,[†,*] James I. Mardel,[‡] Anita J. Hill,[‡] and James E. McGrath[§]

[†]Center for Energy and Environmental Resources, University of Texas at Austin, 10100 Burnet Road, Building 133, Austin, Texas 78758, United States

[‡]CSIRO Materials Science and Engineering, Private Bag 33, South Clayton MDC, Clayton, Vic. 3169, Australia

[§]Macromolecules and Interfaces Institute, Virginia Polytechnic Institute and State University, Blacksburg, Virginia 24061, United States

ABSTRACT: The influence of cation form and degree of sulfonation on free volume, as probed via positron annihilation lifetime spectroscopy (PALS), and water and salt transport properties was determined in a systematic series of directly copolymerized disulfonated poly(arylene ether sulfone) random copolymers. Polymer samples were studied in both the dry and hydrated states. PALS-based estimates of free volume in the dry polymers were compared with those estimated using density and the Bondi group contribution method, and PALS-based free volume data for hydrated polymers were correlated with water and salt transport properties. The transport properties depend strongly on free volume cavity size. Samples with larger free volume elements have higher water and salt solubility, diffusivity, and permeability and lower water/salt diffusivity and permeability selectivity. Sorption of water alters the characteristic free volume of the polymer matrix by two competing mechanisms: water molecules partially occupy the original free volume in the initially dry polymer, thereby reducing free volume cavity size, and water swells the polymer matrix therefore increasing the mean free volume size as a result of increased polymer chain plasticization. The importance of the second effect increases as water uptake and, thus, plasticization increases.

$$FFV = k' \cdot V_F$$

$$D = A \cdot \exp\left[-\frac{\gamma \cdot v^*}{V_F^H}\right]$$

$$P = A \cdot B \cdot V_F^H \cdot \exp\left(-\frac{\gamma \cdot v^*}{V_F^H}\right)$$

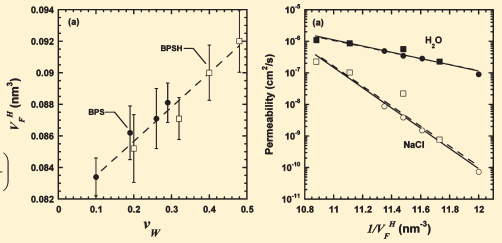

1. INTRODUCTION

Desalination membranes have been studied since the 1950s[1] and have become the technology of choice for brackish and seawater desalination due to their cost effectiveness for this application.[2,3] Cellulose acetate and aromatic polyamides were commercialized for this application.[2−6] However, aromatic polyamide membranes offer higher salt rejection and are stable over wider ranges of feed pH, temperature, and pressure compared to cellulose acetate, so they now dominate the membrane desalination market.[6,7] Nevertheless, polyamides have limited resistance to exposure to oxidizing agents such as chlorine-based disinfectants, which are widely used in water treatment to control biofouling.[6,8,9] To reduce polyamide membrane degradation, water that has been chlorinated to control biofouling must be chemically dechlorinated prior to reaching the polyamide membrane for desalination. To prevent biological contamination, product water is often rechlorinated after desalination.[3,10]

Poly(arylene ether sulfones) exhibit excellent stability in the presence of oxidizing agents such as aqueous hypochlorite, but they are highly hydrophobic, so they are not sufficiently water permeable to be used as separation membranes for desalination.[11] McGrath et al.[12−15] developed techniques to prepare a sulfonated monomer for use in preparing polysulfones, 3,3′-disulfonate-4, 4′-dichlorodiphenyl sulfone. Polymerization methods were developed to incorporate this hydrophilic sulfonated monomer into polysulfones. Via this procedure, directly copolymerized sulfonated poly(arylene ether sulfone) random copolymers (also named biphenol poly(arylene ether sulfone), abbreviated as BPS) were prepared. The hydrophilicity of these polymers can be tailored by varying the content of disulfonated monomer, which results in systematic variations in water and salt transport properties.[16−19]

Free volume plays a central role in determining the transport properties of small molecules in polymers.[20−24] Positron annihilation lifetime spectroscopy (PALS) is a modern tool used to investigate both the size and size distribution of free volume elements in polymers.[25−28] This method is based on the measurement of orthopositronium (o-Ps) lifetime and o-Ps intensity in a material. The annihilation of positrons in a polymer normally occurs via several pathways. One of the pathways, o-Ps pickoff annihilation, is often sensitive to polymer free volume element size and concentration, which are characterized by o-Ps lifetime and intensity, respectively.[29,30] PALS has been used to

Received: December 1, 2010
Revised: April 11, 2011
Published: May 12, 2011

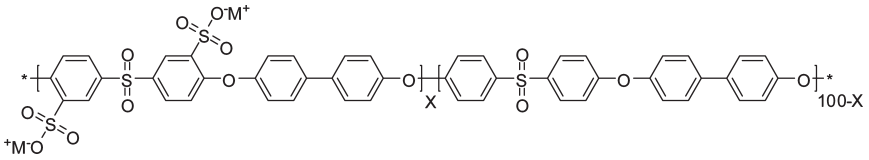

Figure 1. Chemical structure of directly copolymerized disulfonated poly(arylene ether sulfone) random copolymers. The polymers are named as follows: In the BPS-*X* and BPSH-*X* series, *X* = mol % of disulfonated monomer (In our studies, $0 < X < 40$). The BPS-*X* series corresponds to materials originally prepared in the potassium salt form, where M^+ is K^+. The BPSH series corresponds to samples originally prepared in the acid form, where M^+ is a proton.

Table 1. Water and Salt Transport Properties at 25 °C[16,19]

sample	water sorption (volume fraction)	diffusive water permeability[a] (10^{-7} cm^2/s)	NaCl permeability[b] (10^{-9} cm^2/s)	water diffusivity[c] (10^{-6} cm^2/s)	NaCl diffusivity[d] (10^{-7} cm^2/s)
BPS-20	0.10	0.90	0.073	0.90	0.025
BPS-30	0.19	2.8	1.5	1.4	0.38
BPS-35	0.26	3.5	3.9	1.3	1.2
BPS-40	0.29	5.0	8.7	1.7	3.0
BPSH-20	0.20	2.3	0.77	1.1	0.082
BPSH-30	0.32	5.7	22	1.8	4.5
BPSH-35	0.40	8.7	103	2.1	9.8
BPSH-40	0.48	11	226	2.3	20

[a] Measured in a cross-flow system at 25 °C: feed = deionized water; pressure = 400 psig (27.2 atm). [b] Measured using direct permeation cell at 25 °C: donor cell concentration = 1 M NaCl. [c] Calculated from water sorption and water permeability. [d] Measured via kinetic desorption at 25 °C: initially equilibrated in 1 M NaCl.

study the microstructure of various polymers, such as glassy and partially crystalline polymers,[31−33] thermally stable polymers,[34] gas separation polymers,[23,35,36] and polymer hydrogels.[27,37−40] Moreover, free volume, as probed by PALS, correlates well with transport properties in polymeric materials as diverse as gas separation membranes[23,35,36,41] and hydrated polymer hydrogels.[27,40] Desalination membrane materials have also been investigated using PALS.[26,42,43] On the basis of these studies, the positron annihilation technique can probe free volume, which is important in determining penetrant selectivity in reverse osmosis membranes.[26]

In this study, free volume in disulfonated polysulfone films was investigated using PALS. The polymer composition, including the cation form (i.e., acid or salt) and concentration of sulfonated groups, was varied. PALS data from dry samples were compared with free volume results calculated from polymer density and a group contribution method.[44,45] PALS-based free volume in hydrated samples was correlated with water and salt transport properties of these materials.

2. EXPERIMENTAL SECTION

Materials. Disulfonated poly(arylene ether sulfone) random copolymers, whose structure is shown in Figure 1, were prepared by direct aromatic nucleophilic substitution step polymerization, as reported previously.[13,14,46] Dense, uniform, freestanding films (100−150 μm in thickness) of these polymers were prepared by dissolving the polymer (in the potassium salt sulfonate form) in *N*,*N*-dimethylacetamide (DMAc; Sigma-Aldrich, St. Louis, MO; used as received) to form a 10 wt % solids solution. Next, the polymer solution was filtered through a 2 μm pore size stainless steel filter (Cat. nos. SS-2F-2 and SS-2F-K4-2, Swagelok, Solon, OH). After degassing in a vacuum oven at room temperature for 1 h to remove bubbles, the viscous solution was cast onto a clean glass plate. The cast film was first dried in an oven at 80 °C for 24 h, and additional solvent was removed under vacuum for 48 h at 110 °C. Afterward, the film was peeled from the glass plate and stored in deionized water until use. These potassium salt form materials are referred to as the BPS series of materials. To prepare films with the sulfonate groups in the acid form (i.e., the BPSH series of materials), potassium salt form films were boiled in 0.5 M sulfuric acid, which was diluted from 96 wt % sulfuric acid aqueous solution (Fisher Scientific, Hampton, NH; used as received), for 2 h. This step was followed by 2 h of boiling in deionized water to extract excess acid. Finally, the films were dried under vacuum at 110 °C for 24 h before use. This procedure converts the salt form of the polymer (BPS) to the acid form (BPSH).[13,47] Water and NaCl transport properties of these materials are reported elsewhere,[16,18,19] and a summary of the relevant transport parameters is provided in Table 1. The nomenclature for the polymer samples is presented in Figure 1.

Density Determination. The density of dry films was determined using a Mettler Toledo analytical balance (Model AG204, Switzerland) with a Mettler Toledo density determination kit (Part #238490). The measurements were conducted at ambient temperature (24−25 °C). In this hydrostatic weighing method, the polymer density, ρ, was calculated as follows:

$$\rho = \frac{W_d}{W_d - W_l}\rho_l \quad (1)$$

where W_d and W_l are the dry polymer film weights measured in air and in an auxiliary liquid (i.e., a nonsolvent for BPS and BPSH), respectively, and ρ_l is the density of the auxiliary liquid. Cyclohexane (Sigma-Aldrich, St. Louis, MO; used as received) was selected as the auxiliary liquid because sulfonated polysulfones exhibit little affinity for such cyclic alkanes.[48,49]

Positron Annihilation Lifetime Spectroscopy. In this study, PALS measurements were conducted on dry and hydrated BPS and BPSH films. An automated EG&G Ortec fast−fast coincidence system was used to perform PALS measurements. The PALS measurements were performed at ambient temperature with a timing resolution of 240 ps. A thin (2.54 μm), sealed Mylar envelope containing radioactive isotope ^{22}Na was used as the positron source. The Mylar envelope was

Table 2. Density,[18] PALS Results and Free Volume of Dry BPS and BPSH Films

sample	dry density (g/cm^3)	FFV$_\rho$[a] (%)	τ_3^D (ns)	R_F^D (Å)	V_F^D (nm^3)	I_3^D (%)	FFV^{Db} (%)
BPS-20	1.324	16.5	1.961 ± 0.017	2.82 ± 0.02	0.0939	20.1 ± 0.3	3.40
BPS-30	1.349	16.9	1.993 ± 0.018	2.85 ± 0.02	0.0969	19.7 ± 0.2	3.44
BPS-35	1.353	17.5	1.957 ± 0.023	2.81 ± 0.02	0.0929	18.9 ± 0.3	3.16
BPS-40	1.358	18.0	1.901 ± 0.018	2.76 ± 0.02	0.0880	19.1 ± 0.2	3.03
BPSH-20	1.353	12.0	1.943 ± 0.029	2.80 ± 0.02	0.0919	20.0 ± 0.4	3.31
BPSH-30	1.370	11.8	1.924 ± 0.018	2.78 ± 0.02	0.0900	19.3 ± 0.3	3.13
BPSH-35	1.386	11.2	1.894 ± 0.018	2.75 ± 0.02	0.0871	21.3 ± 0.3	3.34
BPSH-40	1.420	9.4	1.829 ± 0.020	2.69 ± 0.02	0.0815	21.7 ± 0.4	3.18

[a] Estimated from density data according to eq 5. [b] Estimated from PALS data according to eq 4.

Table 3. PALS Results and Free Volume of Hydrated BPS and BPSH Films

sample	τ_3^H (ns)	R_F^H (Å)	V_F^H (nm^3)	I_3^H (%)	FFV^{Ha} (%)
BPS-20	1.853 ± 0.013	2.71 ± 0.02	0.0834	19.9 ± 0.4	3.00
BPS-30	1.881 ± 0.016	2.74 ± 0.02	0.0862	16.4 ± 0.2	2.55
BPS-35	1.889 ± 0.020	2.75 ± 0.02	0.0871	16.3 ± 0.3	2.55
BPS-40	1.899 ± 0.014	2.76 ± 0.02	0.0881	15.2 ± 0.2	2.41
BPSH-20	1.871 ± 0.021	2.73 ± 0.02	0.0852	19.5 ± 0.3	3.00
BPSH-30	1.894 ± 0.014	2.75 ± 0.02	0.0871	17.6 ± 0.2	2.77
BPSH-35	1.924 ± 0.024	2.78 ± 0.02	0.0900	16.8 ± 0.6	2.73
BPSH-40	1.939 ± 0.021	2.80 ± 0.02	0.0920	16.7 ± 0.3	2.76

[a] Estimated from PALS data according to eq 4.

sandwiched between stacks of BPS or BPSH films that were at least 1 mm thick. To dissipate electronic charge buildup from ionization of the material, the stack containing the polymer films and the source was wrapped in aluminum foil. The films were dried in a vacuum oven at room temperature overnight prior to PALS measurements, which were performed in a dry N_2 atmosphere. The same dry samples were then equilibrated in deionized water to their fully hydrated state, and the aluminum foil containing the film samples and the positron source were immersed in deionized water for PALS measurements of hydrated BPS and BPSH films. At least five spectra of 30 000 peak counts were collected for each sample. The spectra were analyzed using the PAScual program.[50] This program, based on a finite-term model, fits positron and positronium lifetime and intensity data to a sum of three decaying exponential components (i.e., three lifetimes and intensities).[51] The shortest and intermediate lifetimes were characteristic of parapositronium (p-Ps) self-annihilation and free and trapped positron annihilations, respectively. The p-Ps self-annihilation lifetime was fixed at 0.125 ns, and the free and trapped positron annihilation lifetime was between 0.35 and 0.45 ns.[31] The longest lifetime, τ_3, and its intensity, I_3, were interpreted as the orthopositronium (o-Ps) annihilation signature. These o-Ps components were used to characterize the sample's free volume.[25,30,34,38]

The o-Ps lifetime, τ_3, is longer in larger free volume elements and is used to characterize the free volume element size; the o-Ps intensity, I_3, is often taken to be related to the free volume element density or concentration in a polymer sample.[30] In this study, o-Ps lifetime values were converted to effective free volume element sizes using the traditional semiempirical model based on spherical free volume element geometry:[29,52,53]

$$\tau_3^i = \frac{1}{2}\left[1 - \frac{R_F^i}{R_F^i + \Delta R} + \frac{1}{2\pi}\sin\left(\frac{2\pi R_F^i}{R_F^i + \Delta R}\right)\right]^{-1} \quad (2)$$

Here, τ_3^i is the o-Ps lifetime, R_F^i, is the free volume element radius, i.e., cavity radius, and ΔR is the electron layer thickness, which is set to 1.66 Å.[29,54] The average volume of the free volume elements, V_F^i, was estimated as follows:[29,52,53]

$$V_F^i = \frac{4\pi}{3}(R_F^i)^3 \quad (3)$$

For τ_3^i, R_F^i, and V_F^i, the superscript "i" is "D" for dry samples and "H" for hydrated samples.

In a previous study on hydrated cross-linked poly(ethylene oxide),[27] the fractional free volume (FFV) was proportional to the product of V_F (Å^3) and I_3 (%)[27]

$$FFV = kV_F I_3 \quad (4)$$

where k is a scaling parameter, which had been reported to be 0.018 nm^{-3} for some polymers.[28,55,56] Using o-Ps intensity to characterize the concentration of free volume cavities in other polymers has also been reported in recent publications.[57,58] On the other hand, other studies[59−61] report that electron withdrawing moieties, such as sulfonate groups, can inhibit the formation of o-Ps, which renders I_3 insensitive to changes in free volume element concentration. In this case, eq 4 is no longer applicable for such polymers. This o-Ps inhibition effect also appears to exist for BPS and BPSH polymers, as will be shown in the results below.

3. RESULTS AND DISCUSSION

Density results on dry samples and PALS results from films of these copolymers in both the dry and hydrated states are presented in Table 2 and Table 3, respectively. These films were prepared with various amounts of disulfonated monomer (20 - 40 mol %) in both the potassium salt and acid forms. Characterizing dry samples using PALS assists in understanding the change of PALS parameters upon hydration. Therefore, we report the PALS results in dry samples prior to discussing the results in hydrated samples, although the PALS results for hydrated samples are clearly more relevant for correlating water and salt transport properties.

Before examining the PALS results in detail, it is instructive to first consider the density and fractional free volume, FFV$_\rho$, estimated from density for the dry samples, because this technique is widely used to estimate free volume. Since fractional free volume cannot be measured directly, it is typically estimated using the group contribution method of Bondi:[44,45]

$$\mathrm{FFV}_\rho = \frac{V - V_o}{V} \quad (5)$$

where V is the polymer specific volume, V_o is the specific occupied volume (i.e., the volume which is not available to

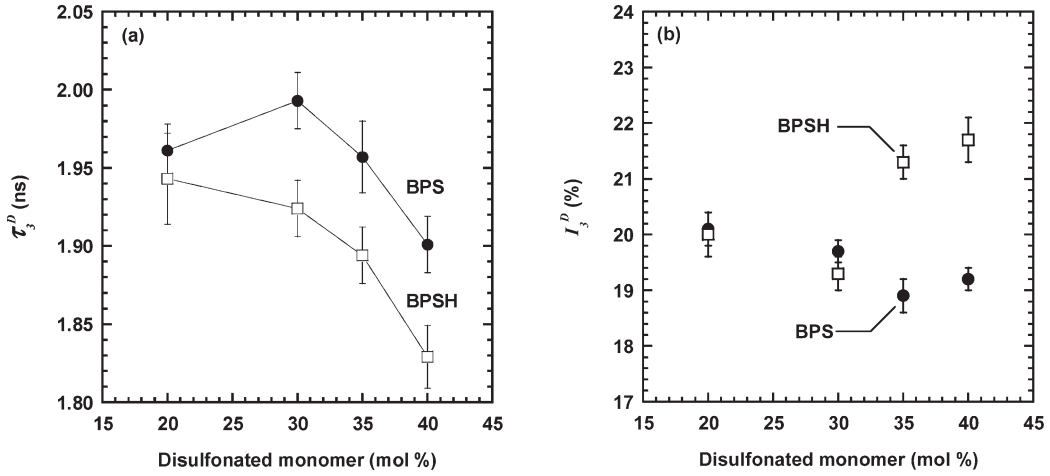

Figure 2. τ_3^D (a) and I_3^D (b) values as a function of sulfonated monomer content in dry samples in the salt (BPS (●)) and acid (BPSH (□)) forms. Error bars are population standard deviations of the results.

assist in penetrant transport). The occupied volume is estimated as follows:

$$V_o = 1.3V_w \quad (6)$$

where V_w is the van der Waals volume of the molecule, typically determined from group contribution methods.[62]

As shown in Table 2, the density of dry BPS and BPSH samples increases regularly with increasing degree of sulfonation. Moreover, the acid form materials are always more dense than their salt form analogues. The FFV_ρ values estimated from the group contribution method are presented in Table 2. From these data, FFV_ρ changes little with sulfonation degree in the salt form materials, but it generally decreases with increasing degree of sulfonation in acid form materials. The FFV_ρ in acid form materials is lower than that in their salt form analogues.

The addition of highly polar sulfonate groups to the aromatic rings of these polymers produces increased intermolecular interaction by pendant ions.[13] The increased interaction would tend to bring molecular segments closer to each other, resulting in more efficient chain packing and decreasing FFV. However, the sulfonate groups are bulky, and the addition of bulky side groups to aromatic polymers, such as polysulfones, often increases free volume.[20,63,64] Thus, as sulfonation level increases, there is potentially a trade-off between increasing chain polarity, which would reduce FFV, and increasing concentration of a bulky substituent, which would increase FFV. Furthermore, salt cations are larger than protons,[65,66] so one might expect the sulfonated salt groups to be bulkier than their acid form analogues, leading potentially to more extensive disruption of polymer chain packing in the salt form materials, which would explain the higher FFV values in salt form materials than in acid form materials. In the salt form materials, the increase in polarity and in the number of bulky substituents as sulfonation level increases largely balance one another, and FFV changes little with sulfonation level. In the acid form materials, the increase in polarity accompanying increasing sulfonation levels is more important than the increase in the number of bulky substituents, so FFV generally decreases as degree of sulfonation increases.

The PALS results on the dry samples, shown in Table 2 and Figure 2, support the previous discussion. Figure 2a presents the o-Ps lifetimes, τ_3^D, as a function of disulfonated monomer concentration. Within the uncertainty of the measurements, the o-Ps lifetime, which characterizes the average free volume element cavity size (eqs 2 and 3), is generally independent of sulfonation levels in the salt form materials, except perhaps for the most highly sulfonated sample, which has a somewhat lower o-Ps lifetime than the other samples. In the acid form materials, the o-Ps lifetime decreases with increasing degree of sulfonation. Furthermore, the free volume element size is generally smaller in the acid form materials than in the salt form materials, consistent with the density and FFV results.

Figure 2b presents the o-Ps intensity, I_3^D. The intensity values are essentially the same in salt and acid form polymers at lower levels of sulfonation (i.e., 20 and 30%) and show some difference at higher degrees of sulfonation, with the intensity being somewhat higher in acid form materials than in salt form materials. While the PALS intensity has often been interpreted as being related to the concentration of free volume elements in polymers, the chemical environment of the polymer can affect o-Ps formation. Positrons interact with electron withdrawing moieties in molecular media, such as sulfonate groups, chloride groups, and bromide groups.[25,61] These electron withdrawing moieties can inhibit the formation of o-Ps, which can render I_3 insensitive to changes in free volume element concentration.[59−61]

Inhibition of o-Ps formation has been used to rationalize sulfonated polymer PALS data. For example, in sulfonated poly(ether ether ketone) with a high degree of sulfonation, the o-Ps intensity was barely detectable, compared to an o-Ps intensity value of 21.2% for unsulfonated poly(ether ether ketone). In sulfonated poly(ether sulfone), the o-Ps intensity exhibits a decreasing trend with increasing sulfonation level.[67] In sulfonated polymers, o-Ps intensity data often do not correlate with transport properties because the o-Ps intensity data are not reflective of the concentration of free volume elements in the polymer. In dry BPS and BPSH polymers, when the concentration of disulfonated groups increases in the acid and salt form samples, there may be conflicting influences on free volume parameters resulting from increasing the number of bulky side groups, which might be expected to increase free volume element concentration, and increasing o-Ps inhibition, which might reduce o-Ps intensity value. The extent to which these factors are controlling in acid and salt form materials may well be different, resulting in the complex behavior exhibited in Figure 2b.

Several studies report the free volume in water-swollen films using PALS. Specifically, Trotzig et al.[40] observed that o-Ps lifetimes

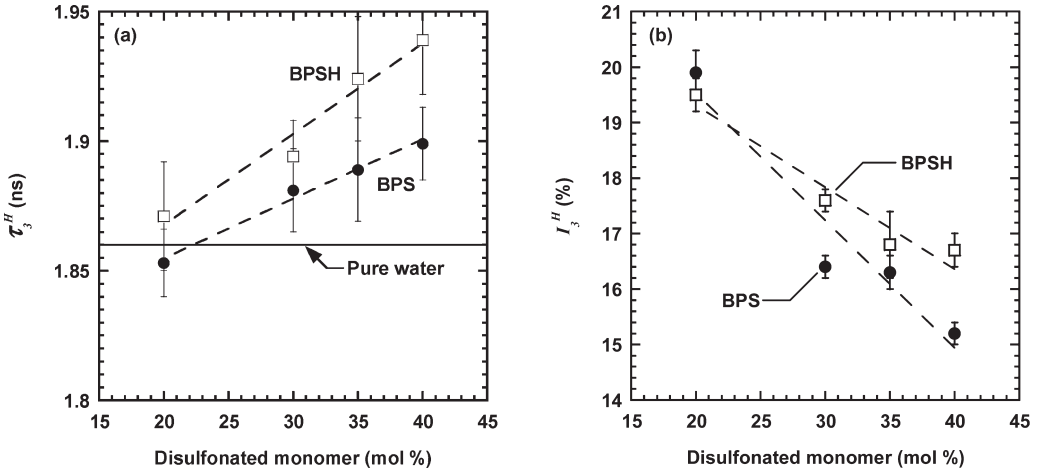

Figure 3. τ_3^H (a) and I_3^H (b) values as a function of sulfonated monomer content in hydrated films of BPS (●) and BPSH (□). Error bars are population standard deviations of the results. The dashed lines are provided to guide the eye.

in PEO films decreased as water content increased in these films, and they ascribed this decrease to the interaction between water molecules and two ether oxygens from different PEO segments, which caused the segments to move closer to one another. In another study, Trotzig et al.[68] reported the presence of water clusters above a water weight fraction of 0.09 w/w in the hydroxypropyl methylcellulose-water system, and the free volume hole size in the plasticized polymer remained constant above a water weight fraction of 0.22 w/w. Sodaye et al.[56] studied the microstructure of Nafion-117 using PALS and reported that the absorption of water decreased o-Ps lifetime in H^+-Nafion. They reasoned that the free volume elements were located in amorphous regions not occupied by water-containing pockets or clusters. Incorporation of water led to expansion of the cluster sizes which could squeeze the amorphous free volume, causing a decrease in mean free-volume element size. However, Hodge et al.[38] showed that as the water content in poly(vinyl alcohol) films increased from 8 to 30 wt %, the inter- and intrachain distances in the polymeric matrix expanded as the polymer swelled, leading to an increase in free volume element size. Thus, the literature shows that addition of water to polymer films can either increase or decrease o-Ps lifetime and, therefore, free volume element size. The PAScal program[50] allows analysis of the data for the fraction of o-Ps annihilating in free water, such as the free water-containing pockets or clusters found in some hydrogels. A free water component with lifetime of ~1.86 ns[69] could not be detected in these studies, indicating that the water in hydrated samples interacts with the polymer.

The PALS results, τ_3^H and I_3^H, for hydrated BPS and BPSH films are presented in Figure 3 as a function of sulfonated monomer content. The trends with increasing sulfonation level are remarkably different from those of the dry films. For example, in Figure 3a, τ_3^H values in both acid and salt form samples increase systematically as degree of sulfonation increases, whereas in the dry samples, they changed little in the BPS series and decreased in the BPSH series with increasing extent of sulfonation (cf., Figure 2a). Previous AFM characterization of these copolymers[13] indicates the presence of cluster-like structures, which are believed to represent hydrophilic sulfonated segments containing small amounts of water. In the hydrated state, these hydrophilic regions can presumably sorb substantial amounts of water. Thus, any inter- and intrachain interactions, which may be substantial in the dry samples due to the presence of the highly charged sulfonate groups, are weakened in the hydrated samples, resulting in the expansion of free volume elements. Therefore, it is not unreasonable that free volume cavity size in hydrated polymers might correlate with the propensity of the copolymers to sorb water. In light of this correlation, the hydrated acid form polymers, which sorb signficantly more water than their salt-form analogues (cf., Table 1), have larger free volume elements than the hydrated salt form polymers, as shown in Figure 3a.

The o-Ps intensity, I_3^H, in both acid and salt forms of these hydrated films decreases with increasing sulfonated monomer content, as shown in Figure 3b. While the intensity values begin at essentially the same value in the 20% sulfonated copolymer, as sulfonation extent increases, the intensity in the acid form materials becomes larger than that in the salt form materials. In the dry films, the o-Ps intensity had the same value in acid and salt forms of the material with 20% and 30% sulfonation, but it increased somewhat in the acid form materials and decreased slightly in the salt form materials, so that the acid form materials had higher o-Ps intensity values in the samples with the highest levels of sulfonation (cf., Figure 2b). Nevertheless, for both salt form and acid form BPS materials, o-Ps intensity inhibition may play a significant role in determining the intensity trend: intensity decreases with increasing degree of sulfonation.

The o-Ps lifetime for pure water, 1.86 ns,[69] is compared to the values observed in these hydrated films in Figure 3a. Additionally, the pure water o-Ps intensity is 27%.[69] The addition of water to the polymer matrix increases the average free volume element size to values above that in pure water. Moreover, the o-Ps intensity in hydrated BPS and BPSH polymers, decreases with increasing degree of sulfonation, moving further away from the value in water, despite the fact that samples with higher degrees of sulfonation contain more water than those of lower degrees of sulfonation. However, due to o-Ps inhibition, the intensity values may have little relation to the concentration of free volume elements in the polymer.

On the basis of the o-Ps lifetime data alone, the addition of water to these materials is doing more than changing free volume by any simple additive mixing rule between the free volume of dry polymer and water. This result is different from that of uncharged hydrogels based on cross-linked poly(ethylene oxide).[27] There, both o-Ps lifetime and intensity generally changed smoothly and regularly between the limits of these parameters in the dry polymer and in water.

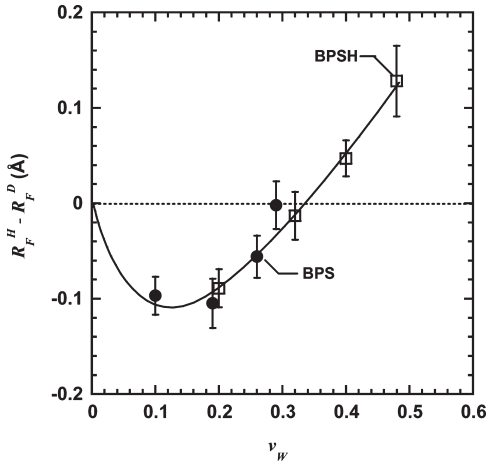

Figure 4. Correlation between water uptake and the difference in free volume element sizes in dry and hydrated films of BPS (●) and BPSH (□). The volume fraction of water sorbed in the samples at equilibrium, v_W.

As degree of sulfonation increases, both BPS and BPSH samples exhibit increases in equilibrium water uptake.[18] Addition of water to the polymer samples may screen the strong inter- and intramolecular interactions that contribute to the decrease in FFV values in the dry acid form samples as sulfonation levels increase. These strong interactions act to maintain FFV at near constant values in dry salt form materials, despite the addition of bulky, potentially packing disrupting potassium sulfonate groups to the chain backbone. Additional evidence for the strong inter- and intramolecular interactions that the sulfonate linkages bring to these polymers in the dry state is provided by the fact that glass transition temperature increases sharply with increasing degree of sulfonation.[13] Therefore, due to the screening effect of the water, the size of free volume elements (i.e., τ_3^H) increases with increasing degree of sulfonation despite the fact that the polymer/water mixture contains higher concentrations of water, which has a lower o-Ps lifetime than that of most of the dry polymers.

It is also of interest to compare the PALS parameters between hydrated and dry acid and salt form samples having the same degree of sulfonation. In this regard, the difference between the free volume cavity size in dry, R_F^D, and hydrated, R_F^H, samples is presented in Figure 4 as a function of the equilibrium volume fraction of water, v_W, sorbed by the hydrated samples. The o-Ps lifetime data were converted to free volume radii values using eq 2. At lower hydration (i.e., $v_W < 0.3$), the size of the free volume elements is smaller in the hydrated samples than that in the dry samples. Then, at higher hydration (i.e., $v_W > 0.3$), the free volume elements are larger in the hydrated samples than that in the analogous dry samples. That is, over the entire range of hydration, the free volume cavity size in the hydrated polymers increases as water uptake increases and finally surpasses the cavity size in the dry polymers. In Figure 4, the difference in free volume element size between dry and hydrated samples was forced through the zero point because there should be no cavity size difference in a sample having no water uptake. Several studies have reported a similar phenomenon for nylon-6.[70−73] Singh et al.[70] and Welander et al.[72] reported the decrease of free volume cavity size at low water uptake. They attributed the reduction in cavity size to the breakage of hydrogen bonds and rearrangement of molecular structure made possible due to the lowering of the glass transition temperature to room temperature in their hydrated polyamides, i.e., the H_2O molecules interrupt the hydrogen bonds leading to high flexibility and hence relaxation of the molecular chains. However, the glass transition temperatures of even fully hydrated BPSH polymers sorbing more water than their salt form analogues have been reported to be higher than 100 °C, and no glass transition was observed below 100 °C in the DSC thermograms.[47] Therefore, the hydrated BPS and BPSH polymers at room temperature are highly glassy and it is unlikely that the molecular structure would experience significant rearrangement upon absorption of water. On the other hand, Robertson et al.[73] found that moisture absorption in nylon-6 is accompanied by an initial decrease in τ_3, attributing this decrease to the occupation of free volume by water molecules; then the free volume cavity size increases when the water sorption level is higher than 10 wt %, which leads to plasticization/swelling of the polymer. In our samples, the initial decrease in free volume cavity size in the hydrated samples may also suggest that water sorbs into the polymer with little or no swelling of the polymer, which effectively decreases the cavity size. Such effects are often observed when small molecules sorb into glassy polymers—at lower concentrations, the small molecules sorb into pre-existing nonequilibrium excess volume sites in the polymer, resulting in a loss of free volume.[74] As water content in the polymer increases, the inter- and intrachain interactions are eventually weakened or screened and, in samples that have the ability to sorb enough water, the polymer chains eventually have the possibility to separate as more water sorbs into the material, thereby generating larger cavity sizes. These hole-filling and swelling effects oppose one another. At low hydration, the hole-filling effect is dominant, so a decrease in cavity size is observed. When the hydration (i.e., water uptake) is beyond about 15 volume percent, the swelling effect becomes dominant, and free volume element size increases with increasing hydration.

The mean free volume element size in the hydrated films, as estimated from the PALS lifetime data and eq 3, is presented in Figure 5(a) as a function of water uptake (i.e., the water sorption values appearing in Table 1). If this parameter is taken as representing the PALS estimate of free volume in these samples, then the free volume as probed by PALS in these hydrated films is linearly proportional to water content. This phenomenon has also been reported for PMMA.[75] Additionally, Yasuda et al.[22] hypothesized that such a relation existed as part of a systematic study of the influence of water content on salt transport in hydrogels. More recently, a similar relation between PALS-based free volume and water uptake was reported in cross-linked PEG-based hydrogels.[27] The difference is that in cross-linked PEG-based hydrogels,[27] the water uptake is proportional to the fractional free volume, which is calculated from PALS-based mean free volume (V_F) and o-Ps intensity (I_3). However, in the BPS and BPSH films, there is a linear correlation between mean free volume size and water uptake. In Figure 5b, the fractional free volume estimated from both the PALS o-Ps lifetime and intensity results (via eq 4) shows no clear trend with water uptake in swollen BPS and BPSH films because the o-Ps intensity values, due to o-Ps intensity inhibition, presumably do not reflect the concentration of free volume elements in the polymer. Therefore, mean free volume element size is a more useful parameter to connect water uptake and PALS-probed free volume for BPS and BPSH films.

Fractional free volume has often been estimated from PALS o-Ps lifetime and intensity as shown in eq 4.[25,27,30] Although PALS information for sulfonated materials exists largely because of the wide use of these materials in fuel cell applications, there is

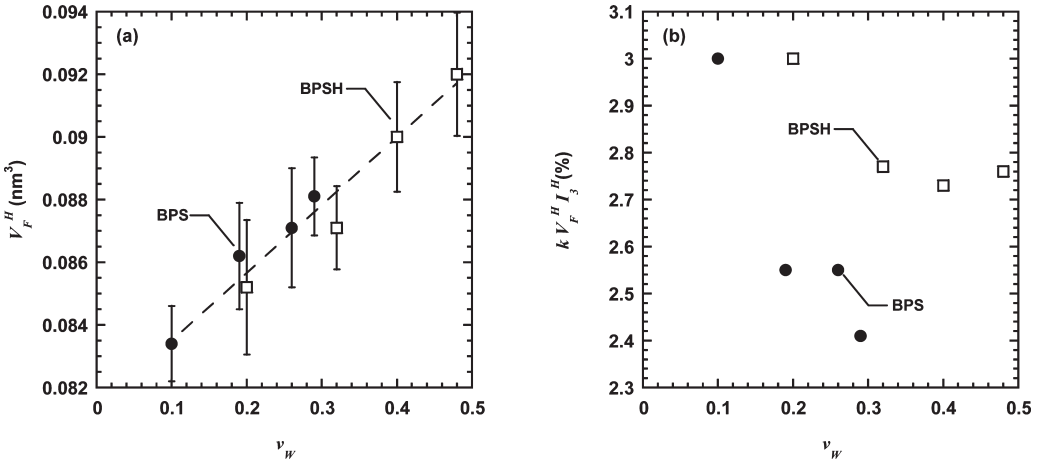

Figure 5. Influence of water uptake (as characterized by the volume fraction of water sorbed by the sample, v_W) on PALS-based: (a) volume of free volume elements and (b) fractional free volume in hydrated BPS (●) and BPSH (□) films. The mean free volume element size and volume were calculated according to eqs 2 and 3, respectively. The dashed line is provided to guide the eye.

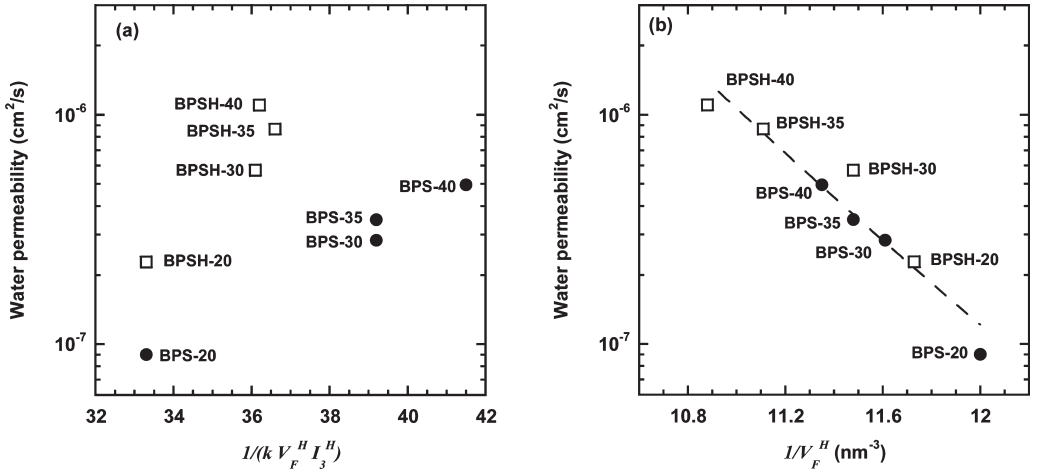

Figure 6. Correlation between diffusive water permeability and (a) reciprocal fractional free volume estimated from eq 4 and (b) average free volume element size, V_F^H, estimated using eq 3 in hydrated BPS (●) and BPSH (□) films.

no evidence of successful correlation between transport properties and o-Ps intensity due to the previously discussed inhibition effect,[23,25,61,67,76] indicating that o-Ps intensity may not be a useful parameter to measure the free volume in this family of polymers. The use of V_F, which is a function of τ_3 only, instead of $V_F I_3$ in eq 4 as a measure of free volume has been reported for other materials.[60,75] Therefore, the fractional free volume in BPS and BPSH films is also taken to be proportional only to the mean free volume size as follows:

$$\mathrm{FFV} = k' V_F \qquad (7)$$

where k' is an empirical proportionality constant.

Membrane transport properties have been reported to be governed by free volume.[22,26,27] Ju et al.[27] showed that, in cross-linked PEG hydrogels, the fractional free volume is well correlated with transport properties such as salt diffusivity. If the fractional free volume of BPS and BPSH films is calculated according to eq 4, this well-established correlation is not observed in the plot of water permeability of these films versus reciprocal fractional free volume (cf., Figure 6a). However, as shown in Figure 6b, water permeability coefficients of BPS and BPSH films are strongly correlated with reciprocal average free volume element size, V_F^H, when the free volume is determined, using eq 3, from PALS o-Ps lifetime values in hydrated samples. If the average free volume in the hydrated polymer is taken to be proportional to the free volume element size in the hydrated state (cf., eq 7), then these results show that permeability varies exponentially with changes in reciprocal average free volume, as expected from free volume theory.[21] The water permeability values of both salt and acid form samples lie on the same trend line with PALS-based reciprocal average free volume element size, indicating that the role of the cation, at least as it applies to water transport, is to influence the water uptake and morphology of the samples, and it is the water uptake that strongly influences free volume and, in turn, water permeability.

The free volume interpretation of diffusion data has been used for both gas separation membranes[35,36,77] and liquid separation membranes.[22,73,78,79] To understand the diffusive permeability of small molecules through hydrated BPS and BPSH films, free volume theory[21,80−83] can be used to correlate the free volume and transport properties. In the discussion that follows, we use

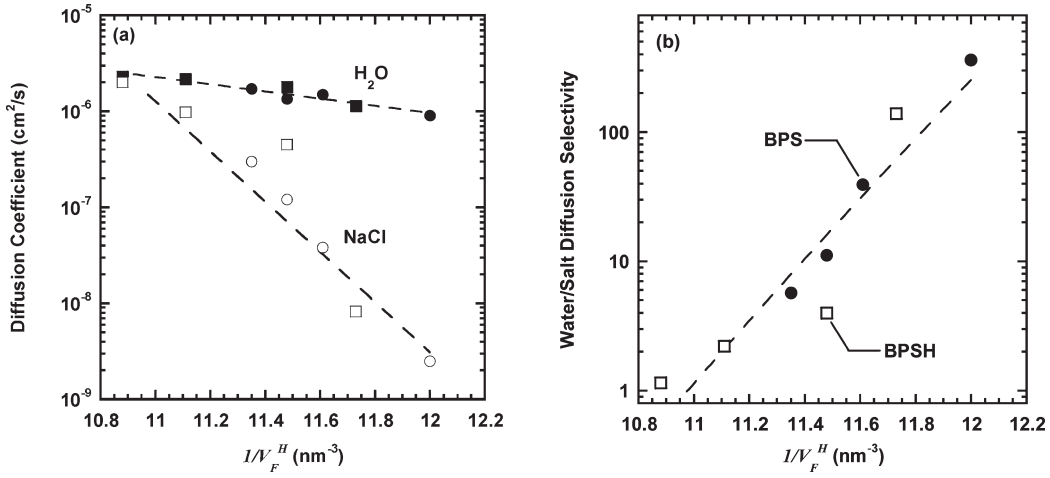

Figure 7. Influence of free volume element size from PALS measurements on: (a) water and NaCl diffusivity and (b) diffusivity selectivity, α_D in BPS (● and ○) and BPSH (■ and □) films. The dashed lines are provided to guide the eye.

average free volume element size in hydrated samples, V_F^H, as a parameter indicative of the average free volume in the polymer. According to the free volume theory and eq 7, small molecule diffusion coefficients in polymers can be correlated with free volume as shown below:[21,83]

$$D = A \exp\left[-\frac{\gamma v^*}{V_F^H}\right] \tag{8}$$

where A is a polymer related constant, γ is a parameter introduced to avoid double counting the free volume elements, and v^* is the characteristic minimum free volume size accessible to the penetrant. v^* depends on the hydrated size of the penetrant. Thus, as penetrant size increases, its diffusion coefficient decreases. In aqueous solution, salt ions exist in a hydrated state with several water molecules surrounding each ion to form a hydrated ion.[84−86] The hydration effect increases the dynamic radius of salt ions, and the size of hydrated ions is larger than that of water molecules.[65,87] Additionally, due to the electroneutrality constraint, each sodium ion that diffuses through a polymer film must have a chloride counterion with it, which means that the effective size of the diffusing species is further increased in the case of the salt.[85] Therefore, the water diffusion coefficient in these copolymer films is expected to be higher than that of sodium chloride. This expectation is verified by diffusion coefficient results presented in Figure 7a. Over the range of sulfonated monomer contents considered, water diffusion coefficients are higher than those of sodium chloride and scale as expected with free volume. As suggested by eq 8, the diffusion coefficients of larger penetrants (NaCl in this case) vary more strongly with changes in free volume than those of smaller penetrants (water in this case). This phenomenon is also observed in Figure 7a because the slope of the line through the NaCl data is steeper than that through the water data.

Free volume cavity size not only determines the diffusion coefficient of penetrants, but it also controls the diffusion selectivity of one penetrant over another. For desalination membranes, it is important to have high selectivity for water molecules over sodium chloride ions to achieve high salt rejection. The diffusivity-selectivity, α_D, of water over salt is defined as follows:[20]

$$\alpha_D = \frac{D_W}{D_S} \tag{9}$$

where D_W and D_S are the water and salt diffusion coefficients, respectively, in the polymer of interest. Substitution of D_W and D_S into eq 9 yields:

$$\alpha_D = \frac{D_W}{D_S} = \exp\left[\frac{\gamma(v_S^* - v_W^*)}{V_F^H}\right] \tag{10}$$

where v_S^* and v_W^* are the minimum free volume element sizes accessible to salt ions and water molecules, respectively. In this work, we equate the minimum free volume element sizes to the volume occupied by one molecule of salt or water in aqueous solution; $v_S^* = 0.192$ nm^3, $v_W^* = 0.010$ nm^3.[88] On the basis of this result, diffusion selectivity should vary exponentially with free volume. Indeed, Figure 7b shows that the water/salt diffusion selectivity of the copolymers considered in this study varies approximately exponentially with free volume element size, as expected. Films with larger free volume elements have lower water/sodium chloride diffusion selectivity but higher diffusion coefficients. This trend is observed because larger penetrants are more sensitive to the size of free volume elements, so the sodium chloride diffusivity increases more rapidly with an increase in free volume cavity size than water diffusivity. This trade-off between rates of transport of water and salt and their selectivity appears to be a general phenomenon in polymers.[88]

In the solution-diffusion model, permeability, P, depends on the product of the solubility of a penetrant in a polymer, K, times the effective diffusivity, D, of that penetrant through the polymer:[89−91]

$$P = KD \tag{11}$$

Introducing eq 8 yields:

$$P = AK \exp\left(-\frac{\gamma \cdot v^*}{V_F^H}\right) \tag{12}$$

According to Figure 5, the water solubility in these polymer films is proportional to the mean free volume size. A previous study[18,19] also showed that the sodium chloride solubility in these copolymers is proportional to water uptake. Therefore, eq 12 can be rewritten as:

$$P = ABV_F^H \exp\left(-\frac{\gamma \cdot v^*}{V_F^H}\right) \tag{13}$$

dx.doi.org/10.1021/ma102745s |Macromolecules 2011, 44, 4428–4438

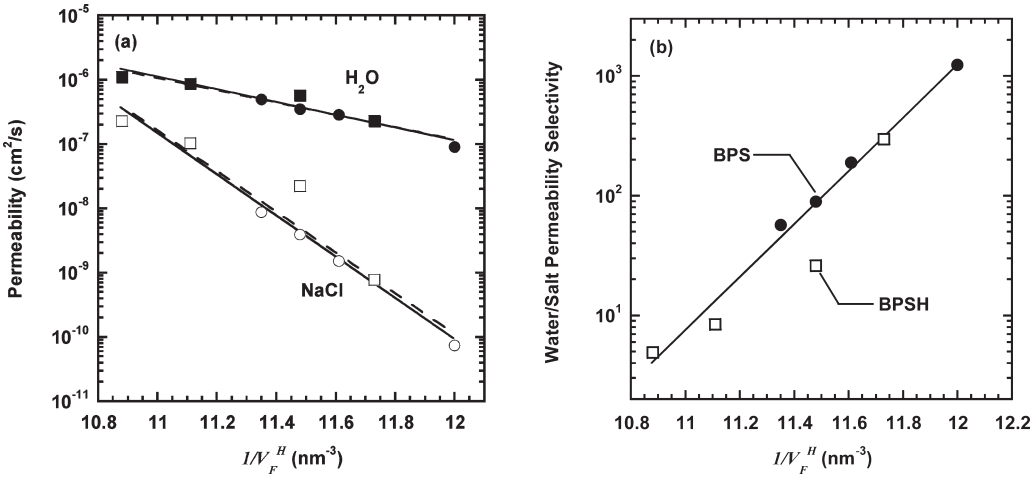

Figure 8. Influence of free volume from PALS experiments on: (a) diffusive water and NaCl permeability and (b) permeability selectivity, α_P, in BPS (● and ○) and BPSH (■ and □) films. The solid lines represent fits of eqs 13 and 14 to the experimental data. For comparison, the dashed lines represent fits of eq 13 to the experimental data by ignoring the term (V_F^H) in eq 13 that is linear in water uptake.

where B is a constant correlating the penetrant solubility of polymer films with the mean free volume element size in the polymer matrix.

The experimental water and sodium chloride permeability data for these copolymer films are presented in Figure 8a as a function of reciprocal free volume element size. The trend is very similar to that observed in the diffusion coefficient data. The solid lines in Figure 8a represent fits of eq 13 to the experimental data. For comparison, the dashed lines show the fits of eq 13 to the experimental data by ignoring the term (V_F^H) that is linear in water uptake. Obviously, the exponential term in eq 13 is dominant and the influence of linear term (V_F^H) is weak enough that the solid lines look to be almost linear.

Permeability selectivity can be expressed as follows:

$$\alpha_P = \frac{P_W}{P_S} = \frac{B_W}{B_S}\exp\left(\frac{\gamma' \cdot (v_S^* - v_W^*)}{V_F^H}\right) \qquad (14)$$

where B_W and B_S are constants related to water and sodium chloride transport in these materials, respectively, P_W is water permeability, and P_S is sodium chloride permeability. Comparison shows that eq 14 is very similar to eq 10. Therefore, a plot of permeability selectivity as a function of average free volume element size (Figure 8b) yields similar trends as those observed in the diffusion selectivity plot (Figure 7b).

4. CONCLUSIONS

PALS results of dry and hydrated BPS and BPSH films were measured and correlated with transport properties. PALS-based free volume element size in hydrated polymers directly correlates with water and salt transport properties. Sorption of water influences the free volume in polymeric films by two mechanisms: hole-filling and swelling. At low hydration, sorbed water molecules occupy pre-existing nonequilibrium free volume elements in glassy polymers. As hydration increases, additional water molecules swell the polymer matrix and subsequently enlarge the free volume cavities. The equilibrium volume fraction of water is proportional to the mean free volume cavity size, indicating that fractional free volume in BPS and BPSH films is strongly correlated with free volume cavity size, as characterized by τ_3. Water and salt diffusivity and permeability of BPS and BPSH films vary exponentially with changes in free volume element size as probed by PALS. Moreover, the diffusion and permeability selectivity increase exponentially as free volume size decreases. Larger free volume cavities lead to higher diffusion and permeability coefficients and lower diffusion and permeability selectivity, and vice versa.

AUTHOR INFORMATION

Corresponding Author

*Telephone: +1-512-232-2803. Fax: +1-512-232-2807. E-mail: freeman@che.utexas.edu.

ACKNOWLEDGMENT

This work was partially supported by the National Science Foundation's Partnerships for Innovation (PFI) Program (Grant No. IIP-0917971) and CBET-0932781/0931761. The authors appreciate CSIRO's Water for a Healthy Country Flagship for their support in conducting the PALS measurements. Additionally, this work was partially supported by the NSF Center for Layered Polymeric Systems (Grant DMR-0423914).

REFERENCES

(1) Loeb, S.; Sourirajan, S. *Adv. Chem. Ser.* **1962**, *38*, 117–132.
(2) Geise, G. M.; Lee, H.-S.; Miller, D. J.; Freeman, B. D.; McGrath, J. E.; Paul, D. R. *J. Polym. Sci., Polym. Chem.* **2010**, *48*, 1685–1718.
(3) Greenlee, L. F.; Lawler, D. F.; Freeman, B. D.; Marrot, B.; Moulin, P. *Water Res.* **2009**, *43*, 2317–2348.
(4) Lonsdale, H. K. *J. Membr. Sci.* **1982**, *10*, 81–181.
(5) Soltanieh, M.; Gill, W. N. *Chem. Eng. Commun.* **1981**, *12*, 279–363.
(6) Petersen, R. J. *J. Membr. Sci.* **1993**, *83*, 81–150.
(7) Cadotte, J. E. *Interfacially synthesized reverse osmosis membrane*. US Patent 4,277,344, 1981.
(8) Knoell, T. *Ultrapure Water* **2006**, *23*, 24–31.
(9) Avlonitis, S.; Hanbury, W. T.; Hodgkiess, T. *Desalination* **1992**, *85*, 321–334.
(10) Nunes, S. P.; Peinemann, K. V., *Membrane Technology in the Chemical Industry*. Wiley-VCH: Weinheim, Germany, 2006.
(11) Robeson, L. M.; Farnham, A. G.; McGrath, J. E. In *Molecular Basis for Transitions and Relaxations*; Meier, D. J., Ed.; Midland

Macromolecular Institute Monographs 4; Midland Macromolecular Institute: Midland, MI, 1978; pp 405−426.
(12) Harrison, W. L.; Hickner, M. A.; Kim, Y. S.; McGrath, J. E. *Fuel Cells* **2005**, *5*, 201–212.
(13) Wang, F.; Hickner, M.; Kim, Y. S.; Zawodzinski, T. A.; McGrath, J. E. *J. Membr. Sci.* **2002**, *197*, 231–242.
(14) Wang, F.; Hickner, M.; Ji, Q.; Harrison, W.; Mecham, J.; Zawodzinski, T. A.; McGrath, J. E. *Macromol. Symp.* **2001**, *175*, 387–395.
(15) Hickner, M. A.; Ghassemi, H.; Kim, Y. S.; Einsla, B. R.; McGrath, J. E. *Chem. Rev.* **2004**, *104*, 4587–4611.
(16) Xie, W.; Park, H. B.; Cook, J.; Lee, C. H.; Byun, G.; Freeman, B. D.; McGrath, J. E. *Water Sci. Technol.* **2010**, *61*, 619–624.
(17) Paul, M.; Park, H. B.; Freeman, B. D.; Roy, A.; McGrath, J. E.; Riffle, J. S. *Polymer* **2008**, *49*, 2243–2252.
(18) Park, H. B.; Freeman, B. D.; Zhang, Z. B.; Sankir, M.; McGrath, J. E. *Angew. Chem., Int. Ed.* **2008**, *47*, 6019–6024.
(19) Xie, W.; Cook, J.; Park, H.-B.; Freeman, B. D.; McGrath, J. E. *Polymer* **2011**, *52*, 2032–2043.
(20) Matteucci, S.; Yampolskii, Y.; Freeman, B. D.; Pinnau, I. In *Materials Science of Membranes for Gas and Vapor Separation*; Yampolskii, Y., Pinnau, I., Freeman, B. D., Eds.; John Wiley & Sons Ltd: Chichester, U.K., 2006; pp 1−48.
(21) Cohen, M. H.; Turnbull, D. *J. Chem. Phys.* **1959**, *31*, 1164–1169.
(22) Yasuda, H.; Lamaze, C. E.; Ikenberry, L. D. *Makromol. Chem.* **1968**, *118*, 19–35.
(23) Mohamed, H. F. M.; Ito, K.; Kobayashi, Y.; Takimoto, N.; Takeoka, Y.; Ohira, A. *Polymer* **2008**, *49*, 3091–3097.
(24) Nagel, C.; Gunther-Schade, K.; Fritsch, D.; Strunskus, T.; Faupel, F. *Macromolecules* **2002**, *35*, 2071–2077.
(25) Pethrick, R. A. *Prog. Polym. Sci.* **1997**, *22*, 1–47.
(26) Shimazu, A.; Ikeda, K.; Miyazaki, T.; Ito, Y. *Radiat. Phys. Chem.* **2000**, *58*, 555–561.
(27) Ju, H.; Sagle, A. C.; Freeman, B. D.; Mardel, J. I.; Hill, A. J. *J. Membr. Sci.* **2010**, *358*, 131–141.
(28) Jean, Y. C. *Microchem. J.* **1990**, *42*, 72–102.
(29) Nakanishi, H.; Wang, S. J.; Jean, Y. C., *Positron Annihilation Studies of Fluids*; World Science: Singapore, 1988; p 292.
(30) Yampolskii, Y.; Shantarovich, V. In *Materials science of membranes for gas and vapor separation*; Yampolskii, Y., Pinnau, I., Freeman, B. D., Eds.; John Wiley & Sons Ltd: Chichester, U.K., 2006; pp 191−211.
(31) Zipper, M. D.; Hill, A. J. *Mater. Forum* **1994**, *18*, 215–233.
(32) Debowska, M. *Acta Phys. Polym, A* **2006**, *110*, 559–568.
(33) Rowe, B. W.; Pas, S. J.; Hill, A. J.; Suzuki, R.; Freeman, B. D.; Paul, D. R. *Polymer* **2009**, *50*, 6149–6156.
(34) Hill, A. J. *ACS Symp. Ser.* **1995**, *603*, 63–80.
(35) Lin, H. Q.; Van Wagner, E.; Swinnea, J. S.; Freeman, B. D.; Pas, S. J.; Hill, A. J.; Kalakkunnath, S.; Kalika, D. S. *J. Membr. Sci.* **2006**, *276*, 145–161.
(36) Lin, H. Q.; Freeman, B. D. *J. Mol. Struct.* **2005**, *739*, 57–74.
(37) Hodge, R. M.; Simon, G. P.; Whittaker, M. R.; Hill, D. J. T.; Whittaker, A. K. *J. Polym. Sci., Polym. Chem.* **1998**, *36*, 463–471.
(38) Hodge, R. M.; Bastow, T. J.; Edward, G. H.; Simon, G. P.; Hill, A. J. *Macromolecules* **1996**, *29*, 8137–8143.
(39) Queiroz, S. M.; Machado, J. C.; Porto, A. O.; Silva, G. G. *Polymer* **2001**, *42*, 3095–3101.
(40) Trotzig, C.; Abrahmsen-Alami, S.; Maurer, F. H. J. *Polymer* **2007**, *48*, 3294–3305.
(41) Wang, X. Y.; Hill, A. J.; Freeman, B. D.; Sanchez, I. C. *J. Membr. Sci.* **2008**, *314*, 15–23.
(42) Garcia, A.; Iriarte, M.; Uriarte, C.; Iruin, J. J.; Etxeberria, A.; del Rio, J. *Polymer* **2004**, *45*, 2949–2957.
(43) Tung, K. L.; Jean, Y. C.; Nanda, D.; Lee, K. R.; Hung, W. S.; Lo, C. H.; Lai, J. Y. *J. Membr. Sci.* **2009**, *343*, 147–156.
(44) Bondi, A. *J. Phys. Chem.* **1964**, *68*, 441–451.
(45) Bondi, A., *Physical Properties of Molecular Crystals, Liquids and Glasses*; Wiley: New York, 1968.
(46) Harrison, W. L.; Wang, F.; Mecham, J. B.; Bhanu, V. A.; Hill, M.; Kim, Y. S.; McGrath, J. E. *J. Polym. Sci., Polym. Chem.* **2003**, *41*, 2264–2276.
(47) Kim, Y. S.; Dong, L. M.; Hickner, M. A.; Glass, T. E.; Webb, V.; McGrath, J. E. *Macromolecules* **2003**, *36*, 6281–6285.
(48) Wohlfarth, C., *CRC Handbook of Enthalpy Data of Polymer-solvent Systems*; Taylor & Francis Group: Boca Raton, FL, 2006.
(49) Madaeni, S. S.; Rahimpour, A. *Polym. Adv. Technol.* **2005**, *16*, 717–724.
(50) Pascual-Izarra, C.; Dong, A.; Pas, S.; Hill, A. J.; Boyd, B.; Drummond, C. J. *Nucl. Instrum. Methods Phys. Res., Sect. A* **2009**, *603*, 456.
(51) Dong, A. W.; Pascual-Izarra, C.; Pas, S. J.; Hill, A. J.; Boyd, B. J.; Drummond, C. J. *J. Phys. Chem. B* **2009**, *113*, 84–91.
(52) Tao, J. *J. Chem. Phys.* **1972**, *56*, 5499–5510.
(53) Eldrup, M.; Lightbody, D.; Sherwood, J. N. *Chem. Phys.* **1981**, *63*, 51–58.
(54) Hill, A. J. In *Polymer Characterization Techniques and Their Application to Blends*; Simon, G. P., Ed.; Oxford University Press: New York, 2003; pp 401−435.
(55) Wang, Y. Y.; Nakanishi, H.; Jean, Y. C.; Sandreczki, T. C. *J. Polym. Sci., Polym. Chem.* **1990**, *28*, 1431–1441.
(56) Sodaye, H. S.; Pujari, P. K.; Goswami, A.; Manohar, S. B. *J. Polym. Sci., Polym. Chem.* **1997**, *35*, 771–776.
(57) Hung, W. S.; De Guzman, M.; Huang, S. H.; Lee, K. R.; Jean, Y. C.; Lai, J. Y. *Macromolecules* **2010**, *43*, 6127–6134.
(58) Lwisnek, L.; Kaushik, M.; Hoyle, C. E.; Nazarenko, S. *Macromolecules* **2010**, *43*, 3859–3867.
(59) Forsyth, M.; MacFarlane, D. R.; Hill, A. J. *Electrochim. Acta* **2000**, *45*, 1243–1247.
(60) Wastlund, C.; Maurer, F. H. J. *Polymer* **1998**, *39*, 2897–2902.
(61) Mallon, P. E. In *Principles and applications of positron & positronium chemistry*; Jean, Y. C., Mallon, P. E., Schrader, D. M., Eds.; World Scientific Publishing Co.: Singapore, 2003; pp 253−280.
(62) Van Krevelen, D. W.; te Nijenhuis, K. *Properties of Polymers: Their Correlation with Chemical Structure; Their Numerical Estimation and Prediction from Additive Group Contributions*; Elsevier: Amsterdam, 2009.
(63) Pixton, M. R.; Paul, D. R. In *Polymeric Gas Separation Membranes*; Yampolskii, D. R. P. a. Y. P., Ed.; CRC Press: Boca Raton, FL, 1994; pp 83−154.
(64) Ayala, D.; Lozano, A. E.; de Abajo, J.; Garcia-Perez, C.; de la Campa, J. G.; Peinemann, K. V.; Freeman, B. D.; Prabhakar, R. *J. Membr. Sci.* **2003**, *215*, 61–73.
(65) Nightingale, E. R., Jr. *J. Phys. Chem.* **1959**, *63*, 1381–1387.
(66) Volkov, A. G.; Paula, S.; Deamer, D. W. *Bioelectrochem. Bioenerg.* **1997**, *42*, 153–160.
(67) Kobayashi, Y.; Mohamed, H. F. M.; Ohira, A. *J. Phys. Chem. B* **2009**, *113*, 5698–5701.
(68) Trotzig, C.; Abrahmsen-Alami, S.; Maurer, F. H. J. *Eur. Polym. J.* **2009**, *45*, 2812–2820.
(69) Eldrup, M.; Mogensen, O. *J. Chem. Phys.* **1972**, *57*, 495–504.
(70) Singh, J. J.; Stclair, T. L.; Holt, W. H.; Mock, W. *Nucl. Instrum. Methods Phys. Res., Sect. A* **1984**, *221*, 427–432.
(71) Heater, K. J.; McDonald, W. F. In *Proceedings of 1992 ASNT Spring Conference, Orlando, FL, 30 March−3 April, 1992*; ASNT: Orlando, FL, 1992; p 175.
(72) Welander, M.; Maurer, F. H. J. *Mater. Sci. Forum* **1992**, *105*, 1815–1818.
(73) Robertson, J. E.; Ward, T. C.; Hill, A. J. *Polymer* **2000**, *41*, 6251–6262.
(74) Fleming, G. K.; Koros, W. J. *Macromolecules* **1986**, *19*, 2285–2291.
(75) Maurer, F. H. J.; Schmidt, M. *Radiat. Phys. Chem.* **2000**, *58*, 509–512.
(76) Mohamed, H. F. M.; Kobayashi, Y.; Kuroda, C. S.; Ohira, A. *J. Phys. Chem. B* **2009**, *113*, 2247–2252.
(77) Lin, H.; Freeman, B. D. *J. Membr. Sci.* **2004**, *239*, 105–117.
(78) Rosenbaum, S.; Mahon, H. I.; Cotton, O. *J. Appl. Polym. Sci.* **1967**, *11*, 2041–2065.
(79) Yasuda, H.; Ikenberry, L. D.; Lamaze, C. E. *Makromol. Chem.* **1969**, *125*, 108–118.

(80) Hirai, N.; Eyring, H. *J. Polym. Sci.* **1959**, *37*, 51–70.
(81) Bueche, F. *Physical Properties of Polymers*; Interscience Publishers: New York, 1962.
(82) Ferry, J. D., *Viscoelastic Properties of Polymers*; J. Wiley & Sons: New York, 1961.
(83) Fujita, H. *Fortschr. Hochpolym. Forsch.* **1961**, *3*, 1–47.
(84) Ohtaki, H.; Radnai, T. *Chem. Rev.* **1993**, *93*, 1157–1204.
(85) Firdaous, L.; Quemeneur, F.; Schlumpf, J. P.; Maleriat, J. P. *Desalination* **2004**, *167*, 397–402.
(86) Rode, B. M.; Schwenk, C. F.; Tongraar, A. *J. Mol. Liq.* **2004**, *110*, 105–122.
(87) Kielland, J. *J. Am. Chem. Soc.* **1937**, *59*, 1675–1678.
(88) Geise, G. M.; Park, H. B.; Sagle, A. C.; Freeman, B. D.; McGrath, J. E. *J. Membr. Sci.* **2011**, *369*, 130–138.
(89) Paul, D. R. *J. Membr. Sci.* **2004**, *241*, 371–386.
(90) Wijmans, J. G.; Baker, R. W. *J. Membr. Sci.* **1995**, *107*, 1–21.
(91) Lonsdale, H. K.; Merten, U.; Riley, R. L. *J. Appl. Polym. Sci.* **1965**, *9*, 1341–1362.